Synthesis of nanoscale titanium dioxide by precipitation using supercritical anti-solvent

I. A. Konovalov,[a] B. N. Mavrin,[b] N. A. Prokudina,[c] and V. V. Fomichev[a]*

[a]*Moscow Technological University (Institute of Fine Chemical Technologies), 86 prosp. Vernadskogo, 119571 Moscow, Russian Federation. E-mail: 9253571868@mail.ru*
[b]*Institute for Spectroscopy, Russian Academy of Sciences, 5 ul. Fizicheskaya, 142190 Troitsk, Moscow Region, Russian Federation*
[c]*Association for Advanced Technologies ASPECT, 86 prosp. Vernadskogo, 119571 Moscow, Russian Federation*

The method of synthesis of nanoscale titanium dioxide from organic precursor using supercritical fluid technology was suggested. It was demonstrated that the obtained product consists of amorphous particles with a narrow size distribution. It possesses a high porosity and a large value of specific surface area. The effect of temperature, pressure, and concentration of the titanium(IV) isopropoxide precursor on the average size of TiO_2 nanoparticles has been studied. The method allows preparation of titanium dioxide free from precursor compounds. Complex physico-chemical study of the obtained product has been performed.

Key words: supercritical fluids, nanoscale titanium dioxide, supercritical anti-solvent method, amorphous TiO_2, highly porous titanium dioxide.

Titanium dioxide possesses unique electrochemical and photocatalytic properties. That makes it an attractive material for various applications. Nanostructured TiO_2 is used as photocatalyst for the decomposition of a wide variety of organic compounds and water splitting, as electrochemical energy storage device, as support for the catalysts, as photoelectrode in the solar cells, as material for the electrochromic devices, as UV filter, and as sensor for different gases.[1—3] Nanosized titanium dioxide is prepared by various methods, such as sol—gel technology, solvo- and hydrothermal processes, electrodeposition, chemical and physical vapor deposition, sonochemical process, micro- and miniemulsion methods, hydrolysis or pyrolysis of $TiCl_4$.[2] It is difficult to obtain meso- and microporous powders using sol—gel technology as the process proceeds slowly.[4,5] Preparation of titanium dioxide having a large specific surface area value (140 $m^2\ g^{-1}$) obtained by a miniemulsion method has been reported.[6] The method allows to adjust the dispersion of the product, however, the phase composition of the resulting material is rather different and represents a mixture of amorphous titanium dioxide with crystalline titanium dioxide in various ratios. Microwave synthesis provides for the rapid progress of the reaction, but results in a wide spread of particle size values.[7] The methods described above have a number of drawbacks associated with the difficulty of adjustment of dispersion, or phase purity, or with a low value of specific surface.[8]

The synthesis method for nanodispersed titanium dioxide by precipitation with supercritical anti-solvent CO_2 (SAS) is suggested in this paper. This method satisfies requirements for the fabrication of a pure product with narrow particle size distribution, high porosity, and large specific surface area value.

The key steps of this method are the following: (1) preparation of the precursor solution in a polar organic solvent; (2) transfer of liquefied CO_2 in a fluid state ($T_{кр}$ = 303.9 K, $P_{кр}$ = 7.38 MPa); (3) contact of fluid with the prepared solution whereby organic solvent dissolves in the fluid and precursor precipitates or decomposes to produce more stable under the experimental conditions substances. The advantages of the method lie in the facts that the process is very fast and the obtained product is of high purity. It is possible to tune finely the size distribution of the product.[9,10]

The synthesis of titanium acetylacetonate by SAS method followed by thermal transformation into titanium dioxide has been described.[11] However, the specific surface area dramatically decreases at thermal treatment, the product transforms into crystalline state and the size of the crystallite is increasing.

Published in Russian in *Izvestiya Akademii Nauk. Seriya Khimicheskaya,* No. 12, pp. 2795–2800, December, 2016.

1066-5285/16/6512-2795

In this work direct single step synthesis of the amorphous titanium dioxide from respective isopropoxide has been carried out.

Experimental

The synthesis was carried out using experimental set-up Super-Particle SAS 50 system (Waters Corp.) (Fig. 1). Gaseous carbon dioxide was cooled in chiller *2* untill temperature of −3 °C, the gas was compressed using high pressure pump *3* (from 8.1 MPa). Afterwards, CO_2 was transferred to heat exchanger *4* (from 35 °C and higher), where the transition in the supercritical state occurred. Initial solution *9* was transferred using isocratic pump *10 via* coaxial nozzle *6* into reactor *5*, where it contacts the fluid. As a result the polar solvent is dissolved in supercritical carbon dioxide. Solid particles are precipitated onto the porous bottom of the reactor *7*, and fluid with dissolved initial solvent is transferred to the cyclone separator *8*, where the pressure is reduced and carbon dioxide is transformed into gaseous state.

The initial solutions were prepared through addition of isopropanol (special grade, ChimMed, TU 2632-011-29483781-09) to titanium tetraisopropoxide (98%, Acros Organic) in different ratio.

Table 1. Experimental conditions

Experiment series	*T*/°C	*P*/MPa	Alcoxide : alcohol /mol mol^{-1}
1	40	7.5, 8.5, 10, 15, 20, 25	1 : 130
2	35, 40, 50, 60, 70, 80	10	1 : 130
3	40	10	1 : 70, 1 : 85, 1 : 100, 1 : 130, 1 : 180, 1 : 250

Then these solutions were transferred into reactor. After the end of the feed of the initial solution into reactor the feed of the fluid was continued for another 15 min to remove the solvent from the surface and from the volume of obtained titanium dioxide. Three series of the experiments were carried out at constant feed rate of CO_2 35 g min^{-1} and feed rate of the initial solution of 0.5 mL min^{-1}. The conditions of the experiments are represented in the Table 1.

X-ray diffraction experiments were carried out using Shimadzu XRD-600 diffractometer (Cu-Kα-radiation, graphite monochromator). ICDD—JCPDS data base was used for phase identification. IR spectra of samples suspended in nujol between two KBr plates were registered using EQUINOX-55 FTIR spectrometer (Bruker). The size of the particles was determined in the sample water suspension by the dynamic light scattering using DelsaNano (Beckman Coulter, Inc.) device. The imaging of the particles was performed using transmission electron microscope JEM-2100 (accelerating voltage 200 kV) and electron microscope JEOL-100CX (accelerating voltage 80 kV). Thermal properties of the samples were analyzed using universal differential scanning calorimeter DSC 204 F1 Phoenix. The content of carbon and hydrogen impurities was determined using Heraeus CHN–O–Rapid analyzer. The content of the gas evolving from the system was analyzed using Agilent 6890N chromatograph. To remove traces of the organic solvent the samples were dried in vacuum oven LT-VO/20 at 0.7 bar. Nitrogen sorption capacity at −196 °C was measured by static volume method in the range of equilibrium relative pressure of nitrogen from 0.01 to 0.99 using ASAP 2020 (Micromeritics) gas analyzer. The samples were degassed in vacuum (residual pressure less than 10^{-3} mm) directly in the measurement tube at 90 °C before measurement. Specific surface area of the samples was determined by the Brunauer—Emmett—Teller (BET) method and by comparative method from the adsorption branch of the isotherm in the area of equilibrium relative nitrogen pressure of 0.05—0.35 and 0.4—0.8, respectively. Raman spectra were excited using 514.5 nm argon laser with power density on the sample of ~100 W cm^{-2}. The investigation of the scattering light was carried out in the reflection geometry. The spectra were analyzed using multichannel spectrom-

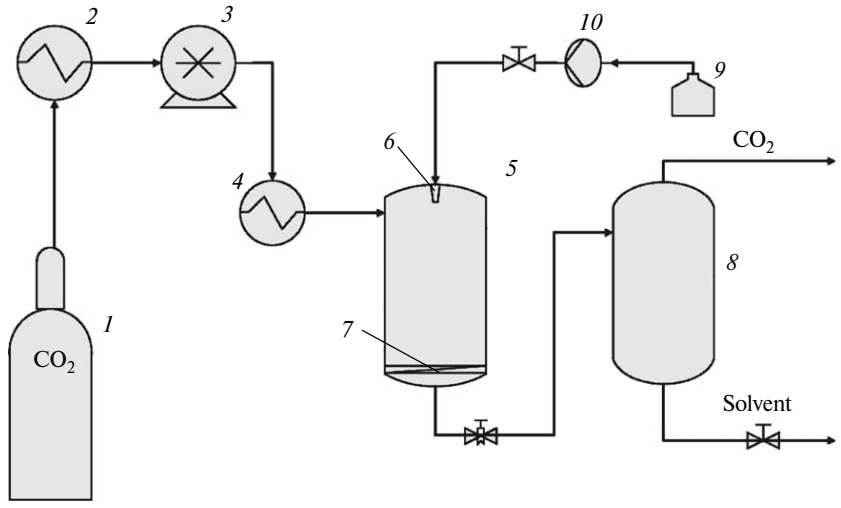

Fig. 1. Principal scheme of SAS set-up: *1*, the CO_2 cylinder; *2*, the heat exchanger (chiller); *3*, the high pressure pump; *4*, the heat exchanger (heater); *5*, the reactor; *6*, the coaxial nozzle; *7*, the porous steel bottom; *8*, the separator; *9*, initial solution; *10*, the isocratic pump.

eter with triple monochromator and resolution of 3 cm^{-1} and CCD-detector of radiation cooled by liquid nitrogen.

Results and Discussion

The results of X-ray diffraction studies show that freshly prepared samples are amorphous. Two clear effects, namely endothermic at 226±3 °C and exothermic at 377±4 °C, are seen in the DSC curves of freshly prepared samples. The thermogram of the sample obtained at the pressure of 15 MPa, system temperature of 40 °C, and molar ratio titanium isopropoxide : isopropanol equal to 1 : 130, is presented in the Fig. 2. Most probably, the first effect represents the process of the removing of the residual solvent.

Along with intensive halo, the peaks corresponding to the anatase crystalline form of the titanium dioxide are observed in the diffractogram of the sample annealed at 340 °C (see Fig. 3). Therefore, partial crystallization occurs.

It was determined using chemical analysis that freshly prepared samples contain admixtures of C (3—5 wt.%) and H (0.5—1 wt.%). It was possible to get rid of these admixtures by drying the samples at 160 °C and 0.07 MPa in vacuum oven for 8 h. Probably, the main admixture was isopropanol adsorbed on the surface and in the volume of particles.

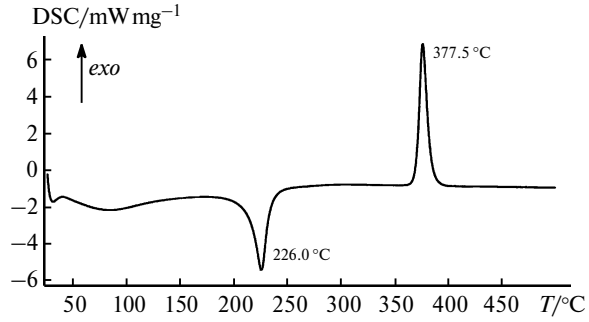

Fig. 2. Thermogram of the TiO_2 sample.

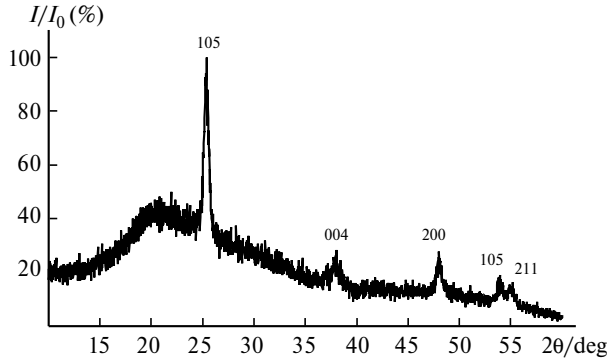

Fig. 3. Diffractogram of TiO_2 annealed at 340 °C for 24 h.

Chromatographic analysis of the gas evolving off the system has shown that along with CO_2 also isopropanol and diisopropyl ester are present. Based on these data the reaction can be represented by the Scheme 1.

Scheme 1

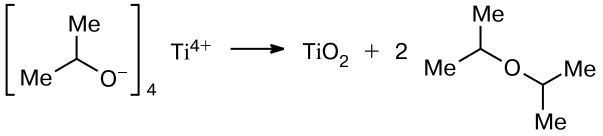

Raman spectra of the samples dried in vacuum at 160 °C and annealed at 340 °C (Fig. 4) are identical and coincide with known Raman spectrum of titanium dioxide with anatase structure. The annealing temperature of 340 °C was selected as highest temperature before exothermic transition of the amorphous substance. Insignificant differences in the spectra of the samples are due to stress in the anatase domains caused by the particles formation in the nonequilibrium conditions with a high speed. The frequency of the intensity band near 152 cm^{-1} is considerably higher than in the anatase crystal (144 cm^{-1}), which can manifest nanodimensions of titanium dioxide crystallites.

It is seen from the microimages that the samples consist mainly of spherical particles (Fig. 5).

Amorphous structure of the samples is clearly seen on the high resolution transmission electron microscopy images (HRTEM). Some areas of ordering are also observed in these images (Fig. 6).

The absence of large number of concentric rings in the image of the electron diffraction (Fig. 7) manifests the amorphous structure of the sample. However, two rings are clearly seen. Therefore, it is possible to conclude on the presence of the areas of ordering.

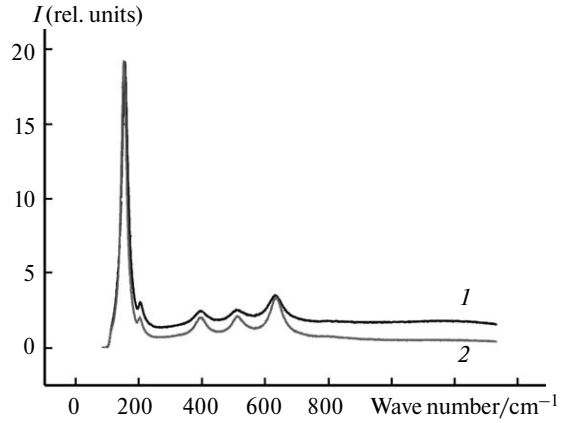

Fig. 4. Raman spectra of TiO_2 dried in vacuum at 160 °C (*1*) and annealed at 340 °C (*2*).

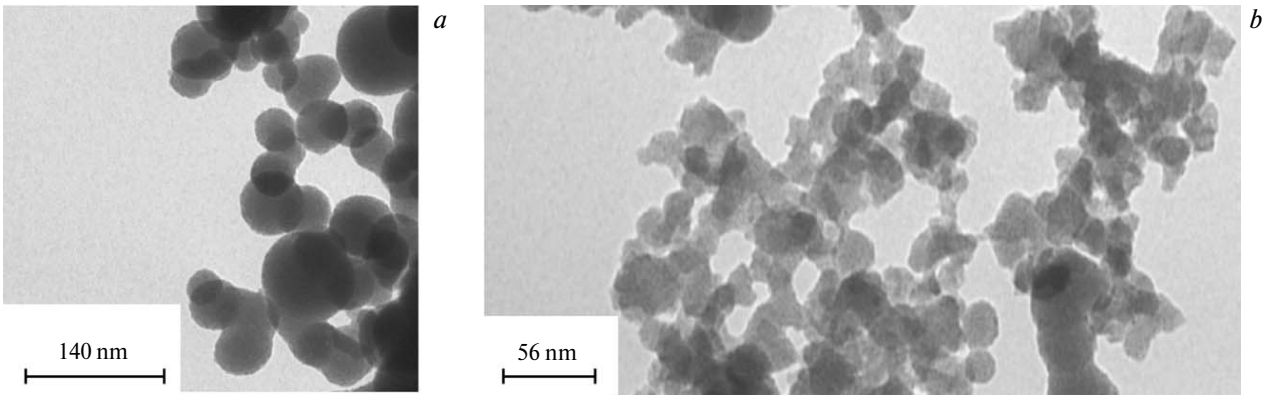

Fig. 5. TEM image of TiO_2 nanoparticles.

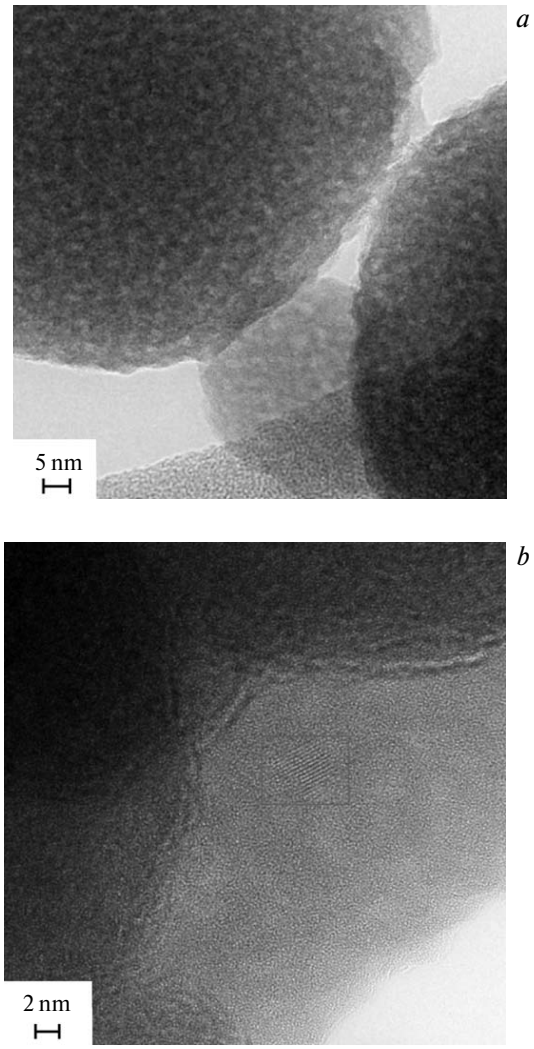

Fig. 6. HRTEM image of TiO_2 nanoparticles.

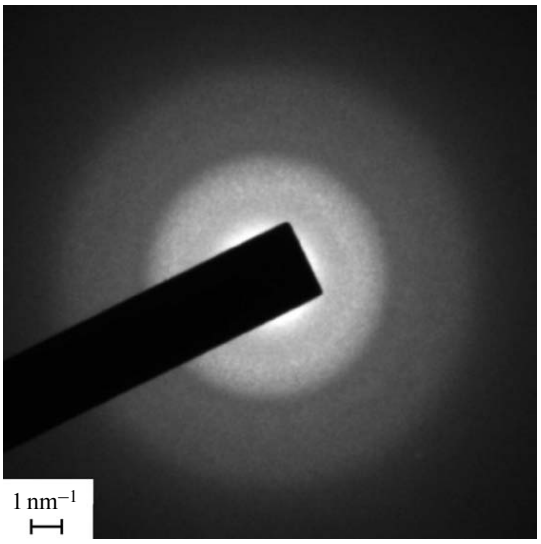

Fig. 7. Electron diffraction of TiO_2 sample (HRTEM method).

Carrying out of three series of the synthesis has allowed to establish the dependence of the average particle size on the experimental parameters. Figure 8 shows the dependence of the average particle diameter of freshly prepared titanium dioxide samples on the pressure, temperature of the synthesis, and the precursor mole fraction. The average particle size is decreased with increasing pressure and temperature, as well as with lowering the mole fraction of titanium(IV) isopropoxide in the solution.

The average size was determined by the dynamic light scattering method. In the sample, freshly prepared at the pressure of 20 MPA, 74% of particle had a diameter of 26 nm, and 26% had a diameter of 31 nm.

Nitrogen sorption isotherm on the surface of amorphous samples *1* (prepared at P = 8.5 MPa, T = = 40 °C, alcoxide : alcohol = 1 : 100 mol mol^{-1}) and *3* (prepared at P = 10.0 MPa, T = 40 °C, alcoxide : alcohol = = 1 : 100 mol mol^{-1}) are assigned according to IUPAC classification[12] to the type I with hysteresis loops of the type H4 and H3, respectively (Fig. 9, *a*). The isotherms of type I are typical for the samples containing ultranan-

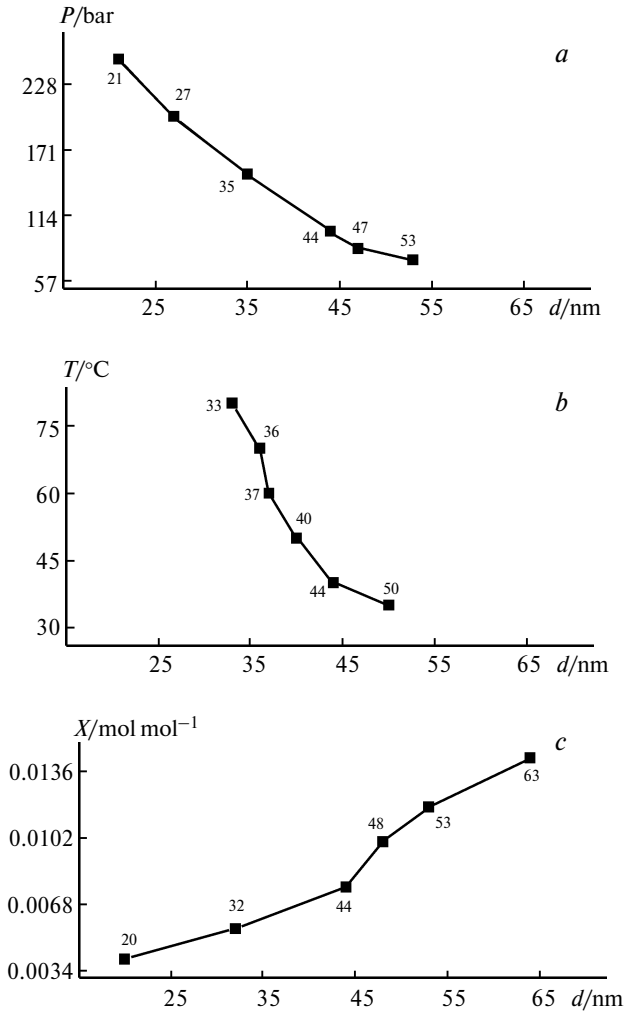

Fig. 8. Dependence of average size of particles on pressure (*a*), temperature (*b*), and molar ratio of titanium tetraisopropoxide in the solution (*c*).

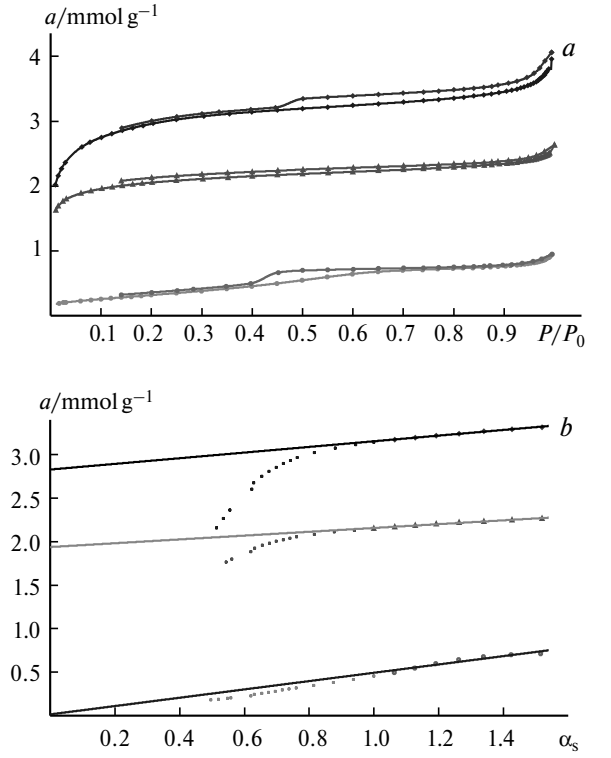

Fig. 9. Isotherms (*a*) and α_s-plots of nitrogen adsorption (*b*) at −196 °C.

opores (pores with the size less than 2 nm, filled with nitrogen according to volume mechanism). The hysteresis loops of types H3 and H4 are typical for the adsorbents containing slit-shaped pores and consisting of plane-parallel particles (H3).[13] The adsorption of nitrogen on the surface of sample *2* (sample *1,* annealed at $T = 450$ °C for 24 h) is described by the isotherm of type II, typical for nonporous samples.[12]

In comparison to the nonporous sample *2* positive segments on the Y-axis (Fig. 9, *b*) due to increased nitrogen sorption in the area of low pressure (see Fig. 9, *a*) are observed for α_s-plots of the samples *1* and *3*. These segments correspond to the volume filling of ultrananopores (pores with diameter less than 2 nm). Negative values of constant C_{BET} (Table 2) also manifest this fact.

The characteristics of the porous texture of titanium dioxide samples are presented in Table 2. The values of the specific surface area of nonporous sample *2,* calculated by BET method and comparison method, practically coincide (27.3 and 28.8 $m^2\ g^{-1}$, respectively), while considerable differences are observed in the values for ultrananoporous samples *1* and *3* (142.4 and 13.2 $m^2\ g^{-1}$ for sample *1*, 209.1 and 19.6 $m^2\ g^{-1}$ for sample *3,* respectively). Total volumes of pores with the size less than 100 nm in the samples *1* and *3* consist of 0.086 and 0.129 $cm^3\ g^{-1}$, respectively. Ultrananopores (the size

Table 2. Porous texture characterization of TiO_2

Parameter	*1*	*2*	*3*
$A_{BET}/m^2\ g^{-1}$	142.4	27.3	209.1
C_{BET}	−49	43	−62
$A_{CM}/\ m^2 g^{-1}$	13.2	28.8	19.6
$V_p/cm^3 g^{-1}$	0.086	0.030	0.129
$V_{un}/cm^3 g^{-1}$	0.059	0.007	0.075
d/nm	40*	18	27*

Notes: A_{BET} is the specific surface area, calculated by BET method, C_{BET} is the BET equation constant, A_{CM} is the specific surface area calculated by the comparison method, V_p is the volume of nanopores (diameter less than 100 nm), V_{up} is the volume of ultrananopores (diameter less than 2 nm). * Calculated value of the average particles size are overestimated due to their aggregation.

less than 2 nm) consist of 69 and 58% of total volume, respectively.

The average size of particles, where layer by layer adsorption of nitrogen occurs, consists of 18 nm for non-porous sample *2*. Calculated values for the samples *1* and *3* consist of 40 and 27 nm, respectively. However, these values are probably overestimated due to inaccessibility for nitrogen of the fraction of the surface of agglomerated particles.

Thus, the synthesis of nanosized amorphous titanium dioxide with high specific surface area (209 $m^2\ g^{-1}$) was successfully carried out by SAS method at temperatures of 35—80 °C and pressure of 7.5—25 MPA. The influence of the preparation conditions on the size of obtained particles has been demonstrated.

References

1. N. Guo, Y. Liang, S. Lan, L. Liu, G. Ji, S. Gan, X. Xu, *Appl. Surf. Sci.*, 2014, **305**, 562.
2. X. Chen, S. S. Mao, *Chem. Rev.*, 2007, **107**, 2891.
3. M. Pelaez, N. T. Nolan, S. C. Pillai, M. K. Seery, P. Falaras, A. G. Kontos, M. H. Entezari, *Appl. Catal. B: Environ.*, 2012, **125**, 331.
4. V. G. Kessler, G. I. Spijksma, G. A. Seisenbaeva, S. Håkansson, D. H. Blank, H. J. Bouwmeester, *J. Sol-gel Sci. Technol.*, 2006, **40**, 163.
5. R. Sui, P. Charpentier, *Chem. Rev.*, 2012, **112**, 3057.
6. R. Rossmanith, C. K. Weiss, J. Geserick, N. Hüsing, U. Hörmann, U. Kaiser, K. Landfester, *Chem. Mater.*, 2008, **20**, 5768.
7. A. B. Corradi, F. Bondioli, B. Focher, A. M. Ferrari, C. Grippo, E. Mariani, C. Villa, *J. Am. Ceram. Soc.*, 2005, **88**, 2639.
8. A. A. L. Chang, PhD Chem. Eng. Diss., North Carolina State University, Raleigh, 2006, 209 pp.
9. R. P. Marin, S. A. Kondrat, R. K. Pinnell, T. E. Davies, S. Golunski, J. K. Bartley, S. H. Taylor, *Appl. Catal. B: Environ.*, 2013, **140**, 671.
10. R. Sui, A. S. Rizkalla, P. A. Charpentier, *J. Phys. Chem. B*, 2006, **110**, 16212.
11. T. Lu, S. Blackburn, C. Dickinson, V. J. Rosseinsky, G. Hutchings, S. Axon, G. A. Leeke, *Powder Technol.*, 2009, **188**, 264.
12. K. S. Sing, *Pure Appl. Chem.*, 1985, **57**, 603.
13. S. J. Gregg, K. S. W. Sing, *Adsorption, Surface Area, and Porosity*, Academic Press, London, 1982, 303 pp.

Received November 26, 2014;
in revised form August 30, 2016